Ice and Snow Feedbacks and the Latitudinal and Seasonal Distribution of Climate Sensitivity

ALAN ROBOCK

Department of Meteorology, University of Maryland, College Park 20742

(Manuscript received 26 May 1982, in final form 3 December 1982)

ABSTRACT

A new parameterization of snow and ice area and albedo as functions of surface temperature is presented based on recent satellite observations of snow and ice extent. This parameterization is incorporated into a seasonal energy-balance climate model. Experiments are conducted with the model to determine the effects of this parameterization change on the latitudinal and seasonal distribution of model sensitivity to external forcings of climate change, such as solar constant variations and changes in the atmospheric carbon dioxide amount.

The sea ice-thermal inertia feedback is found to be the determining factor in this sensitivity pattern, producing enhanced sensitivity in the polar regions in the winter and decreased sensitivity in the polar regions in the summer. The albedo feedbacks (snow-area and snow/ice-meltwater) are weak and produce a small amount of additional sensitivity, but do not change the pattern. The response pattern is the same as that found by Manabe and Stouffer (1980) with a general circulation model. The enhanced sensitivity in the summer found by Ramanathan *et al.* (1979) is shown to be due to a surface albedo feedback parameterization which does not allow the thermal inertia to change. The sensitivity of an annual average version of the model is approximately the same as that of the seasonal model.

1. Introduction

Snow and ice cover increase the surface albedo when they are present. This effect is related to surface temperature, both through the area of the snow and ice, and through the albedo of the snow or ice when present, and is an important climate feedback (Schneider and Dickinson, 1974). In this paper, "snow" will refer to snow cover on land, and "ice" will refer to sea ice. When temperature increases, the snow and ice covers decrease, thus increasing the amount of absorbed solar energy and further increasing the temperature. This will be referred to as the "snow/ice-area feedback." When snow or ice is already present and the temperature is near freezing, if the temperature increases, the albedo will decrease due to meltwater on the surface and changes in the crystal structure, producing a feedback as above. This will be called the "snow/ice-meltwater feedback." The manner in which these feedbacks are parameterized can have a large impact on the sensitivity of a climate model.

During the examination of the above well known albedo feedbacks, another stronger feedback has been discovered. When ice area changes, it also affects the thermal inertia of the ocean-ice-atmosphere system, and this "ice-thermal inertia feedback" will be shown to be dominant in producing the latitudinal and seasonal pattern of climate sensitivity.

The first simple energy balance climate models of Budyko (1969) and Sellers (1969) had a very high sensitivity. When the solar constant (Q) was reduced by 1%, both models produced a reduction of global annual average surface temperature (T_g) of approximately 5°C. A more sophisticated climate model (Sellers, 1973, 1974), which included the seasonal cycle, separate land and water grid boxes, and detailed treatment of the radiative and dynamic heat fluxes, showed a similar high sensitivity in its initial form: a reduction of T_g of 4.65°C for a 1% reduction of Q and an increase of 3.14°C for a 1% increase of Q (Robock, 1979a). General circulation model (GCM) experiments of climate sensitivity to solar constant changes (Wetherald and Manabe, 1975) showed much lower sensitivity, however. Was this difference in sensitivity between the simpler model of Sellers and the GCM due to the Sellers simplified treatment of atmospheric dynamics or some other cause? The experiments in this paper answer this question.

The latitudinal and seasonal distribution of climate sensitivity is of interest in addition to the global, annual average quantities discussed above. Manabe and Stouffer (1980) presented the latitudinal and seasonal distribution of the sensitivity to CO_2 changes. They showed enhanced sensitivity in the polar regions in the winter, which agrees with Mitchell (1961) who found that during the last 100 years climate change was characterized by a much larger sensitivity of the

winter average temperatures than the annual averages. Ramanathan *et al.* (1979) showed a different pattern of sensitivity to CO_2 change with enhanced response in the summer poles. Sellers (1974) also showed enhanced response in the summer. This pattern of sensitivity will be shown to be a strong function of the details of the ice and snow parameterizations.

Robock (1980) showed that not only snow and ice area, but also the surface type of land and the albedo of the snow or ice surface play a large role in determining the surface albedo. When snow lies on a forest the albedo is much lower than when it lies on farming or grazing land. The temperature of the air over a snow or ice cover also affects the albedo by lowering it when the temperature is warmer due to meltwater pockets on the surface and changes in the crystal structure. The earlier energy-balance models did not include these sophisticated effects, and this, it will be shown, contributed to their high sensitivity.

In the next section the new surface albedo parameterization is described. Then, model experiments are presented which show the effects of the different components of the area and meltwater feedbacks on global sensitivity and the latitudinal and seasonal pattern of sensitivity. Finally, the implications of these results are discussed. An Appendix describes minor changes of this climate model from the original Sellers (1973, 1974) version and lists which version of the model was used for different previous studies.

2. Surface albedo parameterization

In an observational study Robock (1980, hereafter referred to as R1) calculated the seasonal cycle of surface albedo based on observations of the seasonal cycles of snow cover and sea ice, and of the distribution of land surface types over the globe. These results are used in this paper as the basis of a parameterization of surface albedo for use in the climate model, as follows. The surface albedo for each 10° latitude band for land or water is calculated using Eq. (4) in R1, which weights the albedo of different surface types by area. The values for the constants are all given in R1. Note that values of F_{b-f}, the fractions of the different land surface types, given in Table 7 in R1 must be divided by F_L, the total fraction of land in each latitude band, to get values to calculate the albedo of land grid boxes. The sea surface albedo is calculated as in Eq. (1) in R1, which includes the solar zenith angle effect. Because R1 found that the effects of clouds and of solar zenith angle are very small in determining the albedo of snow or ice, these effects are not included in this parameterization. The albedos of snow and ice are then calculated as functions of surface temperature as in R1, which gives the meltwater feedback. The land surface temperature is used to determine the albedo of inland ice.

If, in addition, the values of the fractional coverage of sea ice (F_i), inland ice (F_{ii}), and snow (F_s) are known, then the albedo is completely determined. Sellers (1973; hereafter referred to as S) used a parameterization of the following type for snow and ice areas:

$$F = A + BT, \tag{1}$$

where F is the fractional area of snow or ice in a 10° latitude band and T in this case is the temperature 15 days before. In Eq. (1) A is a constant and B is a constant times the annual average temperature (K), and therefore a very weak function of annual average temperature. The values for A and B for snow [S, Eq. (44)] are

$$A = 10.89 \tag{2}$$

$$B = -0.000141\bar{T}_L. \tag{3}$$

When T is expressed in °C, as in this paper, and $\bar{T}_L$ = 273 K, A = 0.52 and B = −0.038. For ice [S, Eq. (42)] the values are

$$A = 8.44 \tag{4}$$

$$B = -0.000110\bar{T}_s. \tag{5}$$

When T is expressed in °C and $\bar{T}_s$ = 273 K, A = 0.25 and B = −0.030. T_L is land surface temperature, T_s is sea surface temperature, and the bar refers to an-

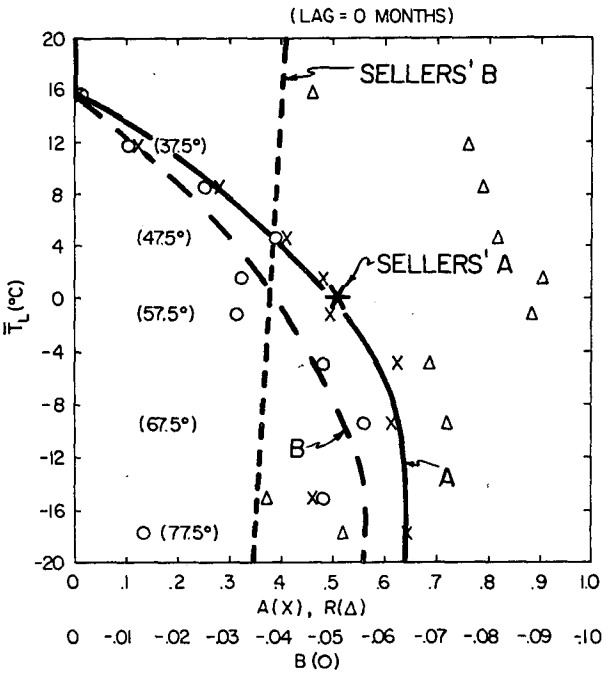

FIG. 1. From Robock (1980, Fig. 22) showing regression coefficients (A, B) plotted as (X, O) and reduction of variance (R) plotted as Δ for Northern Hemisphere snow cover and land temperature observations plotted against annual mean land temperature ($\bar{T}_L$). A and B come from an equation of the form (1). Also plotted are the Sellers (1973) values for A and B from (2) and (3) and this paper's A and B parameterizations from (7) and (8) labeled A and B.

nual average. These values are plotted in Figs. 1 and 2 as functions of annual average temperature. Sellers also included snow on top of the sea ice. The albedo of snow was set at 0.8 regardless of surface type or temperatures, and the albedo of ice was set at 0.6.

In R1, linear regressions of the form (1) were performed from the observations for 5° latitude bands. The highest reduction of variance R was found for snow for a lag of either 0 or +1 months (temperature leading snow) with all the other lags giving much poorer results. For Northern Hemisphere (NH) oceans, the highest R was found at lag +1 (which is really a 1½-month lag with temperature leading ice, because the ice data were for the end rather than the middle of the month) with all other lags giving much poorer results, and for Southern Hemisphere (SH) oceans the highest R was for lag +1 (1 month) with lag +2 slightly lower and all other lags much lower. The resulting regression coefficients are shown in Figs. 1–3 (Figs. 22–24 from R1) plotted as functions of the annual average temperatures for each latitude band.

It can be seen that while the regression coefficients of Sellers agree farily well with the observations when the mean annual temperature is 0°C, they are quite different at other mean annual temperatures. The coefficient A is not constant but varies greatly with $\bar{T}$, and B has a very different functional dependence. Because S had a constant A, he required B to increase with increasing $\bar{T}$, but for the case of snow it actually

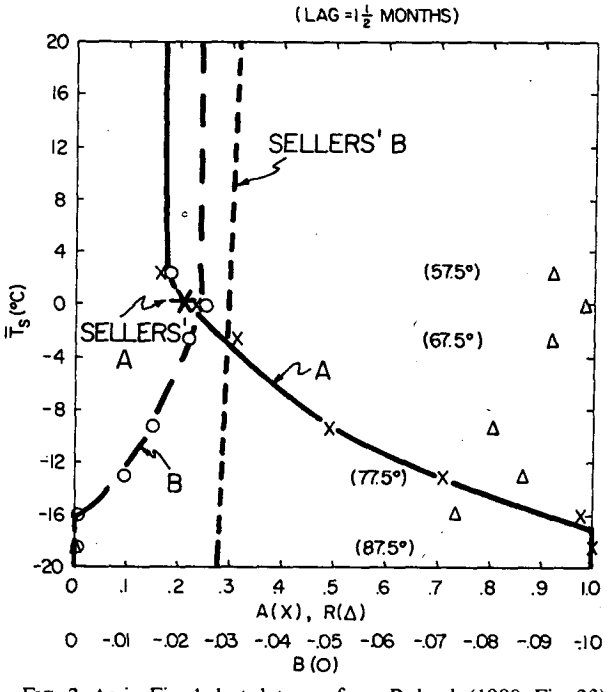

FIG. 2. As in Fig. 1, but data are from Robock (1980, Fig. 23) for Northern Hemisphere sea ice and sea temperature plotted against annual mean sea temperature ($\bar{T}_s$). The Sellers A and B are from (4) and (5) and this paper's A and B are from (10) and (11).

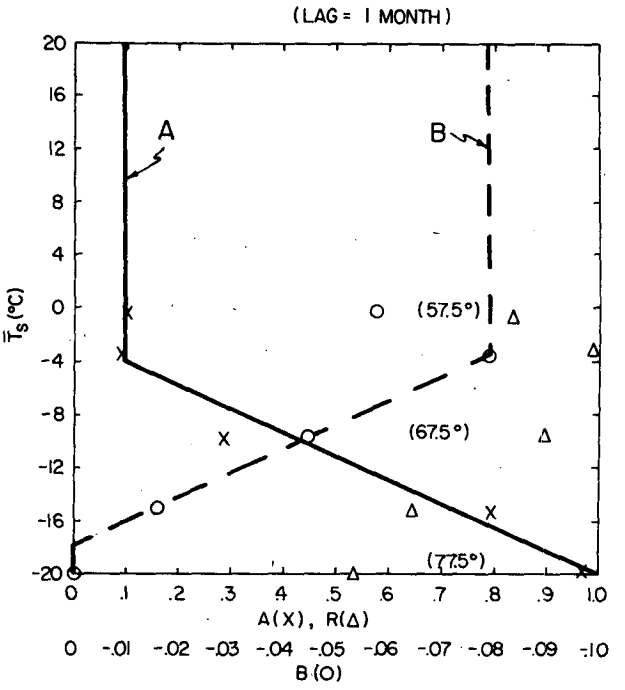

FIG. 3. As in Fig. 2, but for Southern Hemisphere. Data are from Robock (1980, Fig. 24) and A and B curves are from (12) and (13).

decreases. The result for snow is that at low latitudes, the S parameterization gives a mean value much too high, and for high latitudes a value too low. Another difference in the parameterizations is in the temperature-time lag: S used ½ month, while R1 showed that ½ month is appropriate for snow, but 1½ months is correct for ice. In the model climate with the S parameterization (Run 7, 1½ months was used for both snow and ice.

One possibility for a parameterization of fractional area of snow or ice as a function of surface temperature would be to use the values of A and B shown in the figures at each latitude band (suitably averaged from the 5° values given). This would produce an accurate seasonal cycle of snow and ice at each latitude, but would not allow for variations of the A and B coefficients as climate changed. Because of the desirability of having a parameterization with no latitude or time dependent parameters, it was decided to derive relationships for A and B as functions of mean annual temperature, in the way that they seem to depend. Snow and ice areas are thus completely determined by the surface temperature, and change in a realistic way with seasons or on longer time scales.

The A and B values in Figs. 1 and 2 appear to describe parabolic curves with respect to mean annual temperatures, so regressions were performed fitting A and B for snow and ice to functions of mean annual temperature and a constant. For sea ice, the values

from 57.5 to 82.5°N were used in the A regression, and from 62.5 to 82.5°N in the B regression. For snow, the values from 32.5 to 67.5°N were used in both A and B regressions. Cutoffs were required where the curves extended beyond the data. The resulting approximations to A and B are plotted on Figs. 1 and 2 and are described by the equation

$$F_s = A + BT_L(t - 15), \tag{6}$$

where

$$A = 0.63 - 0.0080\,(-12.3 - \bar{T}_L)^2, \tag{7}$$

$$B = -0.062 + 0.000035\,(-28.5 - \bar{T}_L)^2, \tag{8}$$

with the limits:

$$0 \leqslant F_s \leqslant 1,$$

$$B \leqslant 0,$$

$$\bar{T}_L \geqslant -12.3°\text{C}.$$

The reduction of variance is 0.99 for A and 0.90 for B.

For ice,

$$F_i = A + BT_s(t - 45), \tag{9}$$

where

$$A = 0.173 + 0.00172\,(4.9 - \bar{T}_s)^2, \tag{10}$$

$$B = -0.0244 + 0.0000606\,(3.1 - \bar{T}_s)^2, \tag{11}$$

with the limits:

$$0 \leqslant F_i \leqslant 1,$$

$$B \leqslant 0,$$

$$\bar{T}_s \leqslant 3.1°\text{C}.$$

Here, the reduction of variance is 0.95 for A and 0.96 for B. The time t is days and temperatures are °C. The time lags were chosen to correspond to those which produced the best correlations. In Fig. 3, it can be seen that A and B appear to have linear relationships with the annual average temperatures. For the SH ice, therefore, (9) is used, but with

$$A = -0.1250 - 0.05625\,\bar{T}_s, \tag{12}$$

$$B = -0.1028 - 0.005714\,\bar{T}_s, \tag{13}$$

with the limits:

$$\left.\begin{aligned} 0 \leqslant A \leqslant 1 \\ -0.08 \leqslant B \leqslant 0 \end{aligned}\right\}.$$

Curves for these functions of A and B are also plotted on Fig. 3.

By comparing Figs. 2 and 3, and (10) and (11) with (12) and (13), it can be seen that the seasonal cycle of sea ice is different in the two hemispheres. This indicates, as discussed in R1, that physical factors other than surface temperature 1 or 1½ months earlier are responsible for the observed seasonal cycle of sea ice. A correct physically based parameterization should apply equally well in both hemispheres, and would probably include the effects of wind stress, ocean currents, and geography as well as temperature (Andreas and Ackley, 1982). A detailed heat budget for the ice could be developed which would include heat flux through the bottom and carry the ice thickness as a parameter. Such a detailed ice parameterization is beyond the scope of the climate model used here, and so in this study a different parameterization is used for each hemisphere, as described above, with the hope that the physical factors which were excluded do not change significantly with climate. In an experiment to test the importance of this hemispheric assymetry, the NH parameterization was used in both hemispheres, and it did not significantly affect any of the results.

As pointed out by Chernigovskii (1963), and as parameterized in R1, meltwater lowers the albedo of ice and snow when the surface temperature is above freezing. Sellers did not include provisions for this. In early experiments with the climate model using the S parameterization (Version II, see Appendix), the albedo of ice was set to 0.4 when the temperature was above 0°C. In the current versions (III, IV) of the model, the albedo varies as in R1 as a function of the surface temperature, to simulate the meltwater feedback.

3. Results

a. Experimental procedure

In this paper a control run of the climate model is compared to other climate model runs. The control version of the model contains all the changes to the Sellers (1973, 1974) model discussed in Section 2 and the Appendix. That is, it includes the new surface albedo parameterization, the Thompson (1979) planetary albedo parameterization, the cloud data of Berlyand *et al.* (1980), the corrected IR parameterization, and minor changes. Both snow/ice–area feedbacks and snow/ice–meltwater feedbacks are included, but solar zenith angle and cloud effects on snow and ice albedo are not included, because they were previously (R1) found to be very small. Sea ice–meltwater feedback is not used in the SH because meltwater is not observed on SH sea ice (Andreas and Ackley, 1982). The SH sea ice area is calculated from (9), but with A and B determined from SH observations [(12) and (13)].

The control model described above is compared to seven other versions of the model as listed in Table 1. In each case the model is balanced at the current climate, and then 100 year runs are made with Q lowered by 1%, and Q raised by 1%. The global average surface temperature response, and the latitudinal and seasonal distributions of surface temperature response are then compared.

In order for a fair comparison of model sensitivity to be made, it is important to start each experiment at the same climate. When a parameterization in a climate model is changed, and the model is run until it reaches equilibrium, it will reach this equilibrium at a new climate. (In the experiments described here, the model is transitive, except for the unrealistic ice-covered earth solution. After some time, in the absence of stochastic forcing, it reaches an equilibrium with one year exactly duplicating the previous one. The time scale for this process is determined by the average ocean mixed layer depth and is approximately seven years. After 100 years, therefore, virtually no more changes take place.) If the sensitivity of climate is different at different climates, then differences in sensitivity between two versions of a climate model may be due to starting at different climates, rather than to the differences caused by the different parameterizations. In the experiments described here, therefore, each model version is adjusted ("tuned") so that at equilibrium the global average surface temperature is 14.5°C. (Runs 1 through 6 all start at exactly the same climate anyway.) This is accomplished by adjusting the infrared cooling rate parameter (H in Robock, 1979a), and the adjustment is so small that in all cases it equals 1.43°C day^{-1}.

b. Control sensitivity

The global sensitivities of the control model and the other experiments are shown in Fig. 4 and Table 1. For the control, T_g goes up 1.87°C for a 1% increase in Q and down 1.88°C for a 1% reduction in Q. The latitudinal and seasonal distributions of zonal average temperature change for these experiments are shown in Figs 5 and 6. Both experiments produce essentially the same pattern. (Other model experiments in which the atmospheric CO_2 is doubled produce an identical pattern of response.) The sensitivity is higher in the high latitude winter of both hemispheres, extending into the midlatitude spring in the NH. In addition, in the polar summer in the NH, there is a region of lowered sensitivity. It will be shown later that this pattern, is completely produced by the ice and snow feedbacks.

TABLE 1. List of runs, and results of 100-year experiments for Q decreased 1% and Q increased 1%.

	ΔT_g (°C)	
	Q decreased 1%	Q increased 1%
1. Control	−1.88	1.87
2. No albedo feedback	−1.24	1.23
3. Snow area feedback only	−1.29	1.28
4. Ice area feedback only	−1.59	1.60
5. Snow and ice area feedback	−1.68	1.68
6. Snow and ice meltwater feedback only	−1.33	1.32
7. Sellers' surface albedo	−2.49	2.04
8. No seasonal cycle	−2.16	1.83

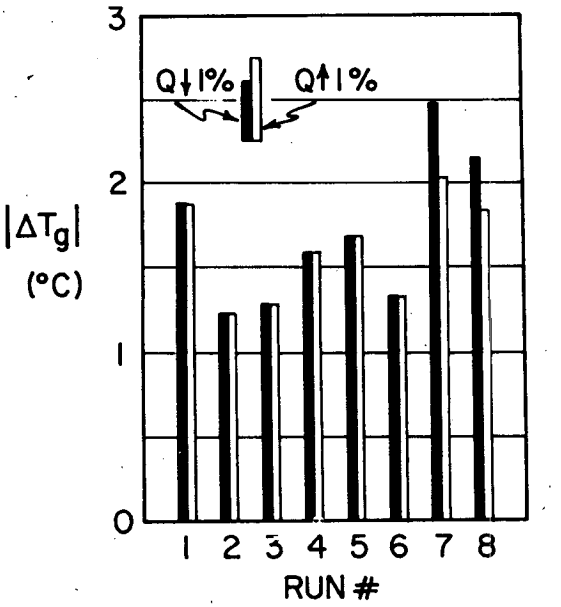

FIG. 4. Change of global average surface temperature (T_g) after 100 years for Q decreased by 1% and Q increased by 1% for the 8 runs listed in Table 1.

The response patterns for Q reduced 1% are presented separately for land and water zonal averages in Figs. 7 and 8. The distributions are quite similar, since they are equilibrium results, and do not reflect the higher ocean thermal inertia (Bryan *et al.*, 1982).

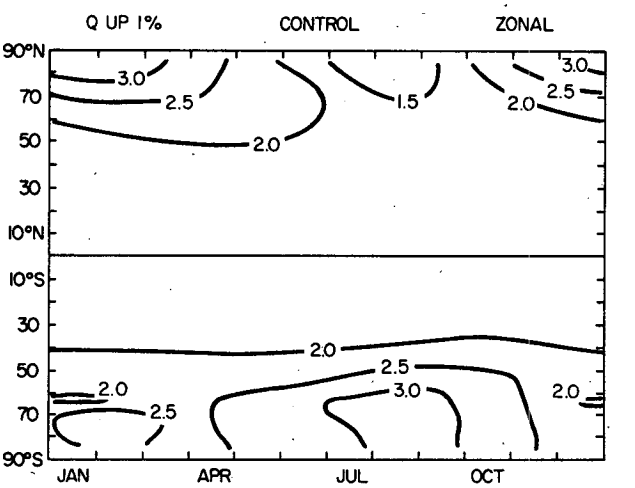

FIG. 5. Change of zonally averaged surface temperature from initial conditions 100 years after Q is raised by 1% for Run 1—Control.

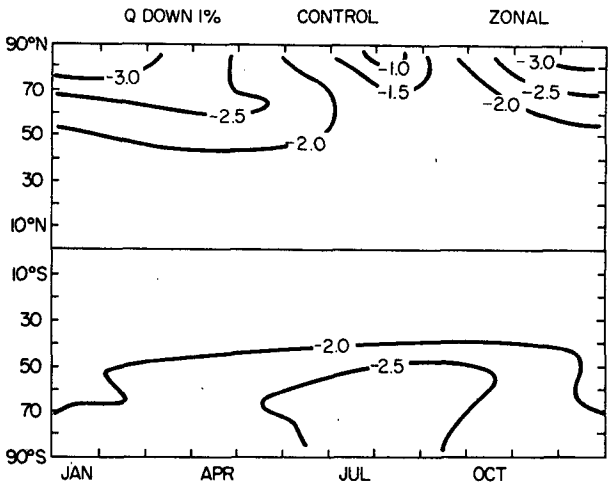

FIG. 6. As in Fig. 5, but for Q lowered by 1%.

It can be noticed, however, that over land in the spring and summer high latitudes in the NH and in the summer near the edge of Antarctica there are regions of enhanced sensitivity due to the snow–albedo feedbacks. In the following discussions, however, due to the similarity of the responses, only zonal average results for Q reduced 1% will be presented.

The results are quite similar to the latitudinal and seasonal distribution of sensitivity shown in the GCM experiment of Manabe and Stouffer (1980) for quadrupling CO_2. The enhanced winter polar response in both hemispheres, the decreased NH summer polar response, the larger winter polar response in the NH compared to the SH, and the region of higher sensitivity on land centered at April, 60°N are features common to both results. Thus, a simple energy balance climate model has reproduced detailed features of the latitudinal and seasonal pattern of response of a complex GCM. An advantage of using the energy balance model for these experiments, is that it uses so little computer time (approximately 100 s of Amdahl 470 V/6 time for a 100 year simulation) that many experiments can be done, as discussed in the next sections, to investigate the reasons for the resulting patterns.

c. *Snow and ice effects*

In this section the effects of snow and ice feedbacks are investigated by using different combinations of the feedbacks.

RUN 2. NO ALBEDO FEEDBACK

In this experiment, no feedback is permitted with snow and ice. Snow and ice albedos and areas are kept fixed at their initial equilibrium values. The results, shown in Table 1 and Fig. 4, show drastically reduced global sensitivity. In addition, the sensitivity to raising Q is almost exactly the same as that for lowering Q, hinting that when nonlinearity in this comparison is found in other experiments, it is due to the snow and ice feedbacks. The value of the sensitivity, 1.24°C, is about what would be expected from only the temperature–radiation and water vapor–greenhouse feedbacks (Cess, 1976). The slight latitudinal–seasonal pattern shown in Fig. 9 (with 0.1°C contours compared to 0.5°C contours in most of the other diagrams) is probably due to the reduced water vapor–greenhouse feedback in the colder regions. The enhancement of sensitivity in the polar regions in the other experiments is therefore due solely to the snow and ice–albedo feedbacks.

In order to further compare the sensitivity in the North Polar region (NP), Fig. 10 gives the seasonal

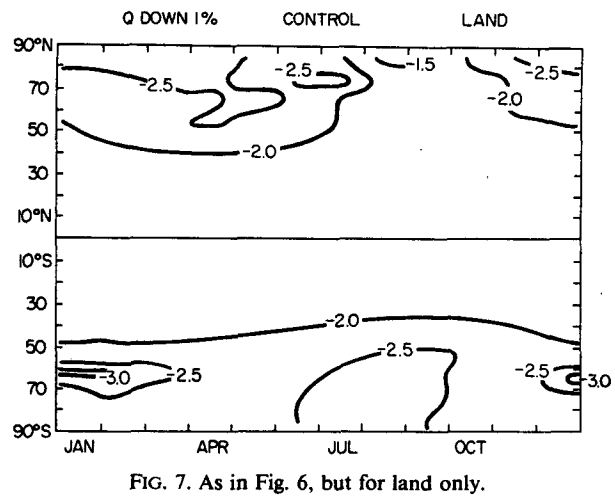

FIG. 7. As in Fig. 6, but for land only.

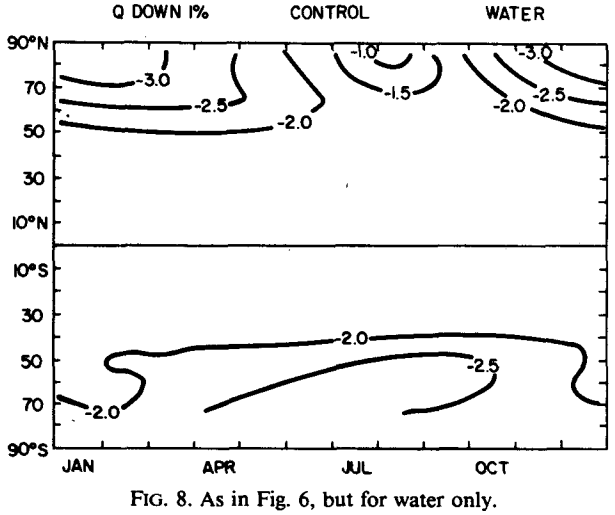

FIG. 8. As in Fig. 6, but for water only.

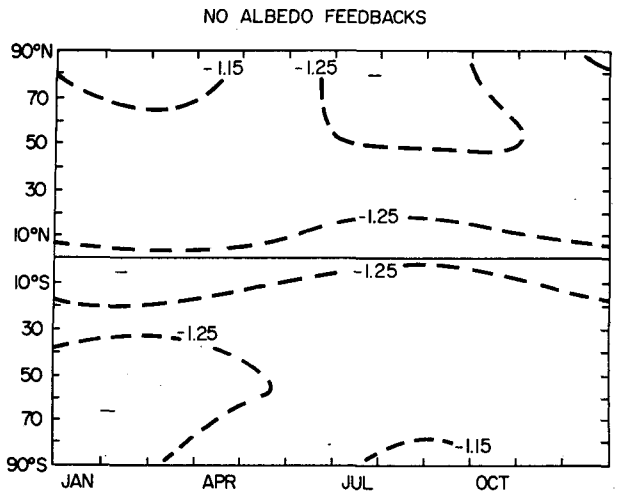

FIG. 9. As in Fig. 6, but for Run 2—No albedo feedback.

cycle of the zonal average temperature deviation for Runs 1–6 for the northernmost latitude band of the climate model, centered at 85°N. The sensitivity of the control is much larger in the winter than Run 2, with no feedbacks, but in summer the control actually has a *lower* sensitivity. This, it will be seen later, is due to the ice–thermal inertia feedback.

RUN 3. SNOW AREA FEEDBACK ONLY

In this experiment, snow and ice albedos and ice area were all fixed at their equilibrium (control) values. Only snow area was allowed to vary, producing an albedo feedback. The global sensitivity, presented in Table 1 and Fig. 4, is only 0.05°C larger for a 1% change of Q. The snow area–albedo feedback is therefore a weak feedback, producing only a 4% increase in global sensitivity compared to a 52% increase for all the snow and ice feedbacks. The latitudinal and seasonal distribution, shown in Fig. 11 (again with 0.1°C contours), is virtually the same as with no snow and ice feedbacks with values slightly higher everywhere but shows an additional slight enhancement in the summer NP. This is the region where this feedback operates, along the snow/no snow boundary when the incoming radiation is large. The seasonal cycle at the NP (Fig. 10) shows the same results.

RUN 4. ICE AREA FEEDBACK ONLY

Only the ice area is allowed to feedback in this experiment, with snow area, and ice and snow albedos kept fixed. The results, Table 1 and Fig. 4, show a large increase in global sensitivity with a latitudinal and seasonal pattern of sensitivity (Fig. 12) that is the same as the control. The lower sensitivity in the summer polar region and much higher sensitivity in the winter pole, also seen in Fig. 10, is caused by this feedback.

When ice area changes, it changes two properties of the system which feed back on the energy balance, the albedo and the thermal inertia. The ice–albedo feedback works the same way as the snow–albedo feedback in the previous run, and by itself would produce the same results. The ice–thermal inertia feedback, therefore, is obviously responsible for the resulting pattern, and it is so strong that it overpowers all the snow and ice albedo feedbacks, and the temperature–radiation and dynamics feedbacks (Schneider and Dickinson, 1974).

The ice–thermal inertia feedback works as follows. When the climate becomes colder, the fractional area of sea ice increases. This reduces the thermal inertia of the system, resulting in a larger seasonal cycle of temperature. As the net radiation reverses sign going from summer to winter, the polar regions cool faster than they would have without this feedback, producing lower winter temperatures. The warming from

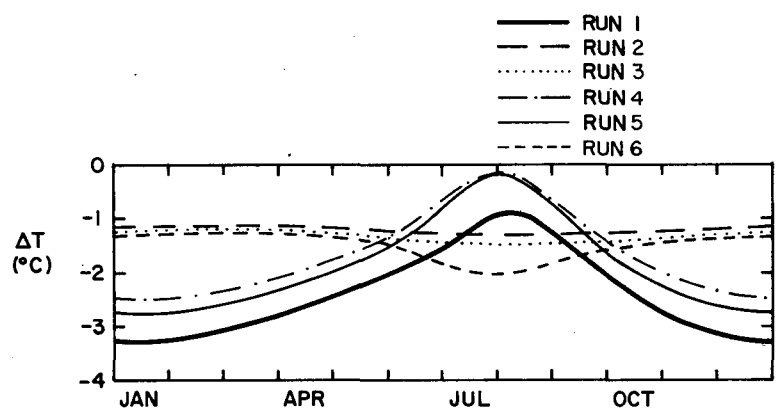

FIG. 10. Seasonal cycle of change from initial conditions after 100 years for zonally averaged temperature in the latitude band 80–90°N. Sensitivity is shown for Runs 1–6.

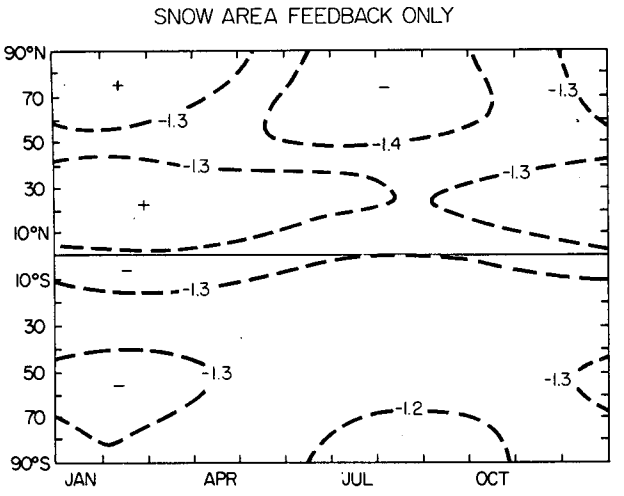

FIG. 11. As in Fig. 6, but for Runs 3—Snow area feedback only.

winter to summer is also larger, with the temperature almost reaching its initial value before Q was reduced. The above analysis applies to the SH and to forcing by warming also. Manabe and Stouffer (1980) attribute the seasonal cycle of sensitivity at the pole to "varying" thermal insulation effects of sea ice. It is seen here that the ice-area feedback works through the thermal inertia effects of sea ice in the same way at all times.

When the pole cools in winter, the north–south temperature gradient increases, tending to produce more northward heat transport which would counteract the cooling. A colder pole would also produce less outgoing IR radiation which would also counteract cooling. More ice in the summer would increase the albedo, tending to make the summer pole cooler than the case with no ice or snow feedbacks. The ice–thermal inertia feedback is so strong that it overpowers all these effects producing the pattern seen in Fig. 12.

RUN 5. SNOW AND ICE AREA FEEDBACK ONLY

In this experiment both snow and ice areas are allowed to feed back, but their albedos are kept fixed, combining the last two runs. The results, seen in Table 1 and Figs. 4, 10 and 13, show the dominance of the ice area feedback, with slightly enhanced sensitivity due to the snow area feedback.

RUN 6. SNOW AND ICE MELTWATER FEEDBACK ONLY

In this experiment, snow and ice areas are kept fixed at their equilibrium values and only the snow/ice–meltwater feedback is operating. The global sensitivity is much lower than for the control, and only slightly higher than for no albedo feedback (Run 2). It is seen in Fig. 14 that the meltwater feedback produces enhanced sensitivity in the summer poles where meltwater occurs and insolation is strong. The effect is larger in the NH, because the model does not allow meltwater on sea ice in the SH.

The seasonal cycle of sensitivity at the NP is shown for this run in Fig. 10. It is seen that although this feedback alone only strongly enhances the sensitivity in the summer at the pole, in combination with the area feedback (Run 5) it produces higher sensitivity in the control (Run 1) as compared to Run 2 in all months equally. This is because with the meltwater feedback alone, thermal inertia is fixed, and the response is a direct one forced only by albedo.

RUN 7. SELLERS' SURFACE ALBEDO

To see the effect of the new surface albedo parameterization, an experiment was run using that of Sell-

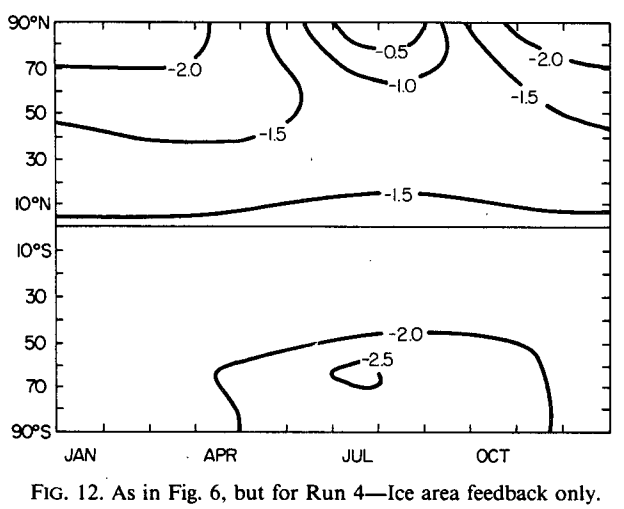

FIG. 12. As in Fig. 6, but for Run 4—Ice area feedback only.

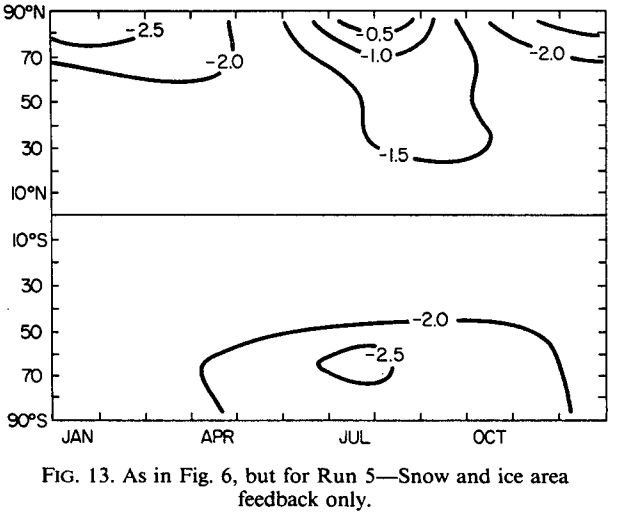

FIG. 13. As in Fig. 6, but for Run 5—Snow and ice area feedback only.

ers (1973). The global average results show that sensitivity is enhanced compared to the control, especially for reducing Q. The latitudinal and seasonal pattern of sensitivity is very different in the NH (Fig. 15). The average sensitivity is larger and there is almost no seasonal dependence, with the largest sensitivity in upper midlatitudes in the summer and at the pole in the spring and summer. The SH, except for having higher sensitivity than the control, has essentially the same pattern. The main differences between this parameterization and the one presented in Section 2 are that in this one the snow albedo is always 0.8 independent of land surface type and the seasonal cycle of snow cover area is too small. The result is that in the summer half of the year there is too much snow and its albedo is too high, creating much more albedo contrast across the snow margin and producing much more sensitivity. In the spring and fall, the high snow albedo by itself produces the enhanced sensitivity. In the SH, there is virtually no seasonal snow, so the summer sensitivity is not enhanced.

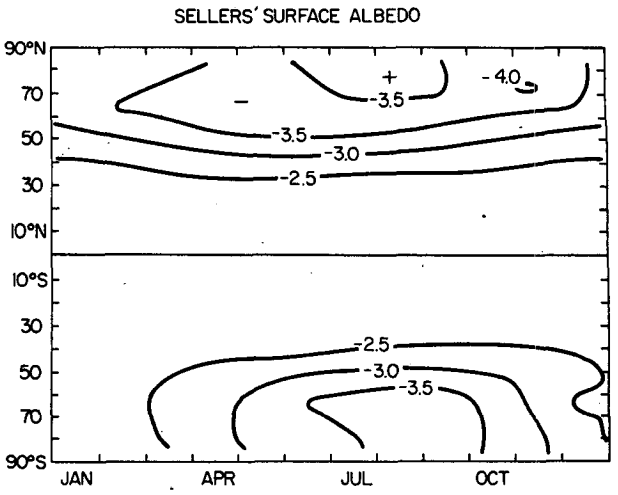

FIG. 15. As in Fig. 6, but for Run 7—Sellers' surface albedo.

RUN 8. NO SEASONAL CYCLE

Many energy balance model experiments have been performed with annual average models. In order to investigate the effects of this simplification on model sensitivity, this experiment simulated an annual average model by fixing incoming solar radiation at its annual average values. The results of this experiment are shown in Figs. 4 and 16. The global sensitivity is lower when Q is raised but higher when Q is lowered, as compared to the control. This behavior is quite similar to the early Budyko (1969) and Sellers (1969) results. The lack of a seasonal cycle puts the average snow line in a region with higher average solar radiation. As solar radiation decreases, the NH snow advances dramatically into a region with a large percentage of land allowing a large area of snow cover. The average radiation here is large, producing the large sensitivity. The opposite is true for increasing Q.

Although the nonlinearity of the response is enhanced, the average sensitivity of the model is approximately the same. The realistic surface albedo parameterization, incorporating observed land uses and their corresponding snow albedos and including the meltwater effect, reduces the albedo contrast at the snow and ice margins. The high sensitivity of the early models, therefore, is due to their unrealistically high snow albedos (0.7–0.8) and not to their lack of a seasonal cycle. The latitudinal pattern (Fig. 16) shows larger sensitivity in the NH compared to corresponding latitudes in the SH, due to the larger snow feedback.

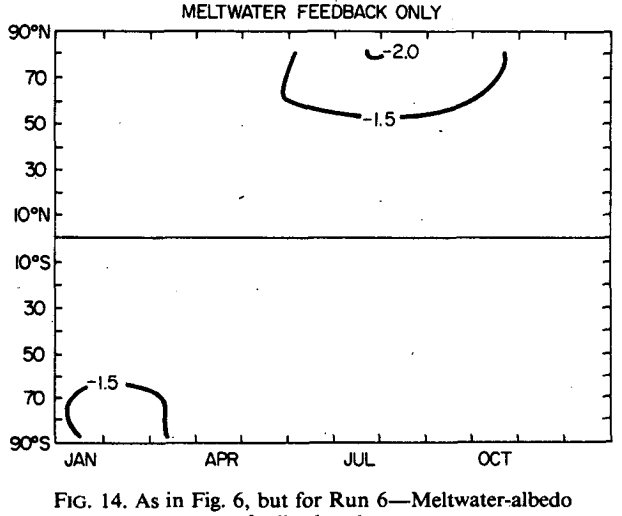

FIG. 14. As in Fig. 6, but for Run 6—Meltwater-albedo feedback only.

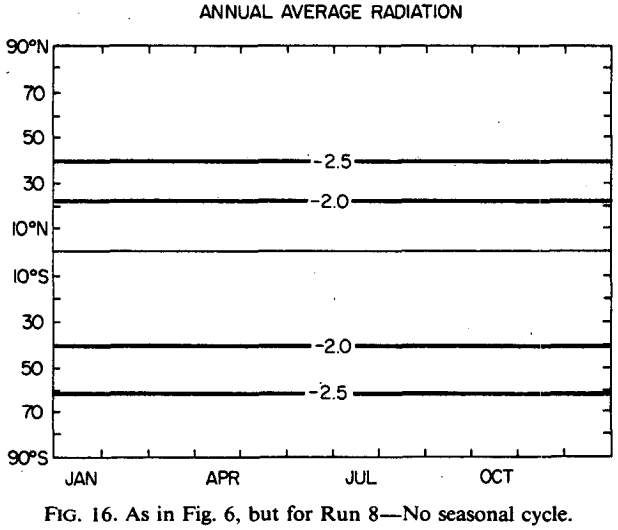

FIG. 16. As in Fig. 6, but for Run 8—No seasonal cycle.

4. Discussion and conclusions

In this paper it has been shown that by using a seasonal energy-balance climate model, ice and snow feedbacks produce enhanced global sensitivity, enhanced sensitivity in the polar regions in the winter, and decreased sensitivity in the polar regions in the summer. The effect is the same for doubling CO_2 or for increasing or decreasing the solar constant. Robock (1981b) found the same response pattern for forcing by transient volcanic dust. It is therefore concluded that, using this climate model, ice and snow feedbacks produce the same characteristic latitudinal and seasonal pattern of response sensitivity for any external forcing, even those which are not globally uniform.

Manabe and Stouffer (1980) found the same pattern of response using a GCM forced with a quadrupling of CO_2. This shows that an energy balance model can reproduce, in great detail, the response of a complex GCM. It is also tempting to conclude from this result that the effects of the ice and snow feedbacks are applicable in all comprehensive climate models, and maybe even the real world.

This conclusion is further strengthened by examining the results of Ramanathan *et al.* (1979). They used a snow/ice parameterization in which the surface albedo was kept constant for surface temperatures above 0°C and only allowed to feed back when the temperature was less than or equal to 0°C. In addition, they did not allow the thermal inertia to change as ice area changed. They found enhanced sensitivity only in the summer near the pole. Their experiment was virtually the same as Run 6 here, which allowed only the meltwater-albedo feedback, which operated when temperatures were between −10 and 0°C. The sensitive areas were the same in both experiments. It is obvious, therefore, that the Ramanathan *et al.* sensitivity pattern is the result of a surface albedo feedback parameterization which ignores the most important part of the feedback, namely the thermal-inertia response. The differences between the Manabe and Stouffer results and the Ramanathan *et al.* results can therefore be explained by differences in their treatment of the snow/ice–albedo feedback.

The ice–thermal inertia component of the ice–area feedback is found to be dominant in producing the resulting latitudinal-seasonal pattern of sensitivity and the enhanced global sensitivity. The albedo components of the snow/ice–area and snow/ice–meltwater feedbacks are strongest in the summer polar region, but the thermal inertia effect overwhelms them.

The albedo parameterizations of Budyko (1969), and Sellers (1969, 1973) all used albedos for snow which did not take into account the very low values found over forested regions or summer meltwater. The albedo contrast between snow and snow-free areas was thus enhanced, producing a stronger albedo feedback and higher model sensitivity. The results found here show that an energy balance model which properly includes the surface albedo will produce the same climate sensitivity as a more complex GCM.

Whether an annual average model is more or less sensitive than a seasonal model is found to depend on the details of the surface albedo parameterization. Using Sellers (1973) parameterizations, Robock (1977) found that the annual average model was more sensitive. It is seen here that the summer sensitivity in the NH with this model (Run 7) is erroneously enhanced due to the wrong snow area and albedo. With a realistic surface albedo parameterization, the sensitivity for an annual average model (Run 8) is approximately the same as for a seasonal model. This result was not found with a GCM by Wetherald and Manabe (1981), who found the annual model more sensitive. The model of Wetherald and Manabe, however, had a seasonal cycle of surface temperature that was too large at the NP. This resulted in the complete absence of snow and ice at the NP in summer, causing no albedo feedback there, and too little in the surrounding months and latitudes, thereby making the seasonal model too insensitive.

In all the above discussion, sensitivity refers to externally imposed climate forcing, such as solar constant or CO_2 changes, or volcanic dust. Actual climate change is caused simultaneously by combined external and internal forcings, and the latitudinal and seasonal distribution of climate response in the real world will depend on the combined and possibly synergistic response to all the forcings. The latitudinal and seasonal distribution of sensitivity to internal (random) forcing may be different than that shown here for external forcing. Borzenkova *et al.* (1976), and Gruza and Rankova (1979) have shown that the observed latitudinal and seasonal pattern of interannual variability of surface temperature has a pattern quite similar to the one found above for external forcing (Figs. 5–8). This pattern of observed variability is the result of a combination of external and internal forcing, and may be due mostly to external forcing. In fact, Kukla and Gavin (1981) found the largest observed temperature changes from 1934–38 to 1974–78 to be *decreases* in the polar winter in the same patterns as shown in this paper and by Manabe and Stouffer (1980). The smaller increases found in the summer pole may be part of the noise and do not validate the Ramanathan *et al.* (1979) results. Interpreting the observed pattern of interannual variability as evidence solely of noise in the climate system may be misleading. The calculation of "signal to noise" ratio by Wigley and Jones (1981) in comparing the observed variability with the response pattern to external forcing, therefore does not give a meaningful result. It is really a "signal to signal + noise" ratio. Additional experiments investigating the latitudinal

and seasonal pattern of sensitivity to internal forcing and to combined internal and external forcing will be necessary before the signal-to-noise ratio can be meaningfully calculated.

Acknowledgments. I thank Claire Villanti for drafting the figures and Caren Klarman for word-processing the manuscript. Calculations were performed on the NASA/GLAS Amdahl computer. This work has been supported by NSF Grant ATM-7918215 and by NOAA Grant NA80-AAD00035.

APPENDIX

Model Versions

Different versions of the Sellers seasonal climate model with different parameterizations and different sensitivities, have been used in different studies (Table A1). This appendix describes each version and specifies the studies in which it was used, in order that the different results can be meaningfully compared.

Version I is the original Sellers Model.

Version II includes changes to the long-wave radiation parameterization and other minor changes. Modifications to the infrared (IR) parameterization of S, as discussed in Robock (1979a), were made to correct an inconsistency. Sellers had assumed that there were no clouds present when calculating the temperatures of two atmospheric layers. He then imposed clouds to calculate the net outgoing infrared flux. The modification assumed clouds present in both instances, a more consistent approach. This somewhat increased the global climate sensitivity.

Sellers had found it necessary to smooth ocean temperature in order to reduce the zonal divergence in high latitudes of the SH [his Eqs. (47) and (48)]. In the calculations here, this was found to be unnecessary, and so was not included. It also was not clear how this correction would reduce zonal divergence, since in the region where S found it necessary, the corrected ocean temperatures were almost equal to their original values. S used one month time steps—12 time steps per year. Using a centered-differencing scheme, this was not enough to accurately resolve the seasonal cycle. Here, 24 time steps per year were used, which is enough to ensure a reasonably small truncation error, and also is convenient for comparing model results to monthly data. Tennekes (1973) showed that the von Karman constant should be 0.35 over smooth surfaces. This value was used instead of 0.40 used by S for ocean surfaces.

This version had a very high global sensitivity and unrealistic seasonal sensitivity distribution, similar to Run 7 in this paper.

Version III incorporated the surface albedo parameterization described in this paper, but used the NH sea ice parameterization for the SH. The sensitivity was slightly larger than for the present control, but the seasonal cycle was correct.

TABLE A1. Model versions and the papers which used them.

Version	Papers
I	Sellers (1973) Sellers (1974)
II	Robock (1977) Robock (1978) Robock (1979a)
III	Robock (1979b) Robock (1981a) Robock (1981b)
IV	this paper

Version IV is the current version, including all the changes described above and the following. The planetary albedo parameterization of Thompson (1979) was used, which explicitly considers zenith angle effects of cloud albedo. In the earlier versions the best available cloud data sets were used, probably similar to those used originally by S. For the SH, data from Sasamori *et al.* (1972) were used; for 0–60°N, the data of London (1957); and for the north polar regions, the data of Vowinckel and Orvig (1970). These data sets were all zonally averaged and had very poor seasonal resolution. A new data set (Berlyand *et al.*, 1980) has become available which gives monthly average cloudiness of 10° latitude bands separately for land and ocean. Since this is the same resolution as the climate model, this improved data set was used, with values interpolated at half-month intervals. Fractional cloud amounts were kept fixed, with no feedback. Berlyand *et al.* use mostly surface observations to derive their cloud climatology. Satellite observations are still too ambiguous to give a reliable global cloud climatology, and the direction and strength of the cloud-climate feedback have not been established. The new planetary albedo parameterization produced sensitivity which was slightly lower than Version III. The change in clouds had little effect.

Fig. 2 of Robock (1981b) presents results of an experiment with snow and ice kept at their model climatological values. This was the same as Run 6 in the current paper, with meltwater–albedo feedback only. The regions of enhanced sensitivity found in the summer poles in that experiment were thus due to the meltwater feedback. Experiments conducted since then, with no albedo feedback, resulted in no seasonal or latitudinal variation of sensitivity in response to volcanic forcing, as in Run 2.

REFERENCES

Andreas, E. L., and S. F. Ackley, 1982: On the difference in ablation seasons of Arctic and Antarctic sea ice. *J. Atmos. Sci.*, **39**, 440–447.

Berlyand, T. G., L. A. Strokina and L. Ye. Greshnikova, 1980: Zonal cloudiness distribution over the globe. *Meteor. Hydrol.*, No. 3, 15–23.

Borzenkova, I. I., K. Ya. Vinnikov, L. P. Spirina and D. I. Stekhnovskiy, 1976: Change in air temperature in the Northern Hemisphere during the period 1881–1975. *Meteor. Hydrol.*, No. 7, 27–35.

Bryan, K., F. G. Komro, S. Manabe and M. J. Spelman, 1982: Transient climate response to increasing atmospheric carbon dioxide. *Science,* **215,** 56–58.

Budyko, M. I., 1969: The effect of solar radiation variations on the climate of the earth. *Tellus,* **21,** 611–619.

Cess, R. D., 1976: Climatic change: An appraisal of atmospheric feedback mechanisms employing zonal climatology. *J. Atmos. Sci.,* **33,** 1831–1843.

Chernigovskii, N. T., 1963: Radiational properties of the central Arctic ice coat. *Tr. Arkt. Antarkt. Nauchno-Issled. Inst.,* **253,** 249–260.

Gruza, G. V., and E. Ya. Rankova, 1979: *Data on the Structure and Variability of Climate. Air Temperature at Sea Level. Northern Hemisphere.* USSR State Comm. Hydrometeor. and Control of the Natural Environment, 203 pp. [Available from Dr. G. V. Gruza, All-Union Research Institute of Hydrometeorological Information—World Data Center, Obninsk 249020, USSR.]

Kukla, G., and J. Gavin, 1981: Summer ice and carbon dioxide, *Science,* **214,** 497–503.

London, J. L., 1957: *A Study of the Atmospheric Heat Balance. Final Report.* Contract AF 19(122)-165, College Eng., New York University, 99 pp. [NTIS No. PB115626].

Manabe, S., and R. J. Stouffer, 1980: Sensitivity of a global climate model to an increase of CO_2 concentration in the atmosphere. *J. Geophys. Res.,* **85,** 5529–5554.

Mitchell, J. M., Jr., 1961: Recent secular changes of global temperature. *Ann. N.Y. Acad. Sci.,* **95,** 235–250.

Ramanathan, V., M. S. Lian and R. D. Cess, 1979: Increased atmospheric CO_2: Zonal and seasonal estimates of the effect on the radiation energy balance and surface temperature. *J. Geophys. Res.,* **84,** 4949–4958.

Robock, A., 1977: Climate predictability and simulation with a global climate model. Ph.D. thesis, MIT, 219 pp. [Available from Dept. Meteor., MIT, Cambridge, Massachusetts 02139.]

——, 1978: Internally and externally caused climate change. *J. Atmos. Sci.,* **35,** 1111–1122.

——, 1979a: The performance of a seasonal global climatic model. *Report JOC Study Conf. Climate Models: Performance, Intercomparison and Sensitivity Studies,* W. L. Gates, Ed., GARP Publ. Ser. No. 22, WMO/ICSU, 766–802.

——, 1979b: The "Little Ice Age": Northern Hemisphere average observations and model calculations. *Science,* **206,** 1402–1404.

——, 1980: The seasonal cycle of snow cover, sea ice, and surface albedo. *Mon. Wea. Rev.,* **108,** 267–285.

——, 1981a: A latitudinally dependent volcanic dust veil index, and its effects on climate simulations. *J. Volcanol. Geotherm. Res.,* **11,** 67–80.

——, 1981b: The Mount St. Helens volcanic eruption of 18 May 1980: Minimal climatic effect. *Science,* **212,** 1383–1384.

Sasamori, T., J. London and D. V. Hoyt, 1972: *Radiation Budget of the Southern Hemisphere. Meteor. Monogr.,* No. 35, Amer. Meteor. Soc., 9–23.

Schneider, S. H., and R. R. Dickinson, 1974: Climate modeling. *Rev. Geophys. Space Phys.,* **12,** 447–493.

Sellers, W. D., 1969: A global climatic model based on the energy balance of the earth–atmosphere system. *J. Appl. Meteor.,* **8,** 392–400.

——, 1973: A new global climatic model. *J. Appl. Meteor.,* **12,** 241–254.

——, 1974: A reassessment of the effect of CO_2 variations on a simple global climatic model. *J. Appl. Meteor.,* **13,** 831–833.

Tennekes, H., 1973: The logarithmic wind profile. *J. Atmos. Sci.,* **30,** 234–238.

Thompson, S. L., 1979: Development of a seasonally-verified planetary albedo parameterization for zonal energy balance climate models. *Report JOC Study Conf. Climate Models: Performance, Intercomparison and Sensitivity Studies,* W. L. Gates, Ed., GARP Publ. Ser. No. 22, WMO/ICSU, 1002–1023.

Vowinckel, E., and S. Orvig, 1970: The climate of the North Polar Basin. *World Survey of Climatology,* Vol. 14, H. Landsberg, Ed., Elsevier, 129–252.

Wetherald, R. T., and S. Manabe, 1975: The effects of changing the solar constant on the climate of a general circulation model. *J. Atmos. Sci.,* **32,** 2044–2059.

——, and ——, 1981: Influence of seasonal variation upon the sensitivity of a model climate. *J. Geophys. Res.,* **86,** 1194–1204.

Wigley, T. M. L., and P. D. Jones, 1981: Detecting CO_2 induced climatic change. *Nature,* **292,** 205–208.